THE JOURNAL OF BIOLOGICAL CHEMISTRY
Vol. 279, No. 45, Issue of November 5, pp. 46764–46771, 2004
Printed in U.S.A.

Improved Lymphocyte Function-associated Antigen-1 (LFA-1) Inhibition by Statin Derivatives

MOLECULAR BASIS DETERMINED BY X-RAY ANALYSIS AND MONITORING OF LFA-1 CONFORMATIONAL CHANGES *IN VITRO* AND *EX VIVO**

Received for publication, July 14, 2004, and in revised form, August 6, 2004
Published, JBC Papers in Press, August 10, 2004, DOI 10.1074/jbc.M407951200

Gabriele Weitz-Schmidt‡, Karl Welzenbach, Janet Dawson, and Joerg Kallen‡

From the Novartis Institutes for BioMedical Research, CH-4002 Basel, Switzerland

The integrin lymphocyte function-associated antigen-1 (LFA-1) ($\alpha_L\beta_2$; CD11a/CD18) plays an important role in leukocyte migration and T cell activation. LFA-1 is inhibited by the cholesterol-lowering drug lovastatin, which binds to an allosteric site of the α_L I domain termed the lovastatin site (L-site). Here we report for the first time the x-ray structures of the LFA-1 I domain complexed with derivatives of lovastatin optimized for LFA-1 inhibition. This analysis identified two new subpockets within the L-site occupied by chemical groups of the statin derivatives but not by lovastatin itself. Occupancy of these L-site subpockets led to distinct conformational changes in LFA-1, which were detectable by an epitope-monitoring assay. We utilized this assay to demonstrate improved LFA-1 inhibition in human blood *in vitro* and in blood samples from treated animals *ex vivo*. Moreover, we demonstrate that the novel lovastatin-derived LFA-1 inhibitor LFA878 exhibits potent anti-inflammatory effects in carrageenan-induced rat paw edema. In summary, the findings reported here extend the understanding of LFA-1 inhibition at the molecular level, allow for the identification and design of LFA-1 inhibitors of further enhanced potency, and support the expectation that LFA-1 inhibitors binding to the L-site will be of therapeutic value in treating inflammatory diseases.

Lymphocyte function-associated antigen-1 (LFA-1)[1] ($\alpha_L\beta_2$; CD11a/CD18) is a α/β heterodimeric receptor belonging to the β_2 integrin subfamily. LFA-1 resides on leukocytes in a low affinity, non-ligand binding state. The integrin requires activation by divalent metal cations or intracellular signals in order to bind to its major counter receptor, intercellular adhesion molecule (ICAM)-1, expressed on both endothelial cells and leukocytes (1). As a member of the β_2 integrin family LFA-1 contains an inserted (I) domain located between the β-sheets 2 and 3 of a seven-bladed β-propeller region on the α_L chain (2). Within the I domain a divalent cation coordination site (named metal ion-dependent adhesion site or MIDAS) interacts directly with the Glu-34 of ICAM-1 (3). The β_2 chain of LFA-1 contains an I-like domain that is known to regulate the activity status of the α_L I domain during LFA-1 activation. In contrast to the α_L I domain, the β_2 I-like domain does not participate directly in ligand binding (4, 5).

LFA-1 plays a major role in lymphocyte homing and leukocyte trafficking in inflammation (1). In addition, as a component of the immunological synapse, LFA-1 is involved in T cell activation upon antigen recognition (6). These multiple functions make LFA-1 a promising therapeutic target in inflammatory and immunological diseases. Indeed, clinical studies suggest that anti-LFA-1 antibody therapy may be beneficial in bone marrow and solid organ transplantation (7, 8). The most convincing clinical data to date has been reported for a humanized anti-LFA-1 mAb administered to patients with chronic plaque psoriasis (9). However, the use of biologicals poses significant limitations in clinical practice, *e.g.* the need for parenteral application. Thus the availability of orally active low molecular weight inhibitors of LFA-1 would be highly desirable.

High throughput screening has identified various low molecular weight inhibitors of the LFA-1/ICAM-1 interaction (10). Based on their mode of action, these inhibitors can be divided into two major classes. The α I allosteric inhibitors have been shown to bind to a hydrophobic pocket near the C-terminal helix α_7 of the α_L I domain but distant from the MIDAS (10–16). By binding to this pocket, the LFA-1 inhibitors are thought to block a downward axial displacement of helix α_7, which is critical for I domain activation (10).

In addition to this first group of inhibitors, a second group of LFA-1 inhibitors has been recently identified that are thought to bind to the MIDAS of the β_2 I-like domain, thereby affecting both the β_2 I-like and α_L I domain (17, 18). These inhibitors, termed α/β I-like allosteric inhibitors, appear to disrupt signal transmission between the LFA-1 I domain and the I-like domain, resulting in a default low affinity conformation of the I domain (10, 18).

The 3-hydroxy-3-methylglutaryl coenzyme A reductase inhibitor lovastatin belongs to the class of α I allosteric inhibitors that interact with the hydrophobic pocket near the C-terminal helix α_7 of the I domain (11, 12). Because lovastatin was the first molecule shown to bind to this site, the site was termed the lovastatin site (L-site) (12). A series of lovastatin derivatives has since been synthesized that inhibit LFA-1 more potently than lovastatin itself and do no longer affect the activity of 3-hydroxy-3-methylglutaryl coenzyme A reductase (12, 17). Little is known about the molecular basis leading to improved LFA-1 inhibition by these compounds. Moreover, most of the studies addressing LFA-1 inhibition by low molecular weight

* The costs of publication of this article were defrayed in part by the payment of page charges. This article must therefore be hereby marked "*advertisement*" in accordance with 18 U.S.C. Section 1734 solely to indicate this fact.

The atomic coordinates and structure factors (code 1XDD and 1XDG) have been deposited in the Protein Data Bank, Research Collaboratory for Structural Bioinformatics, Rutgers University, New Brunswick, NJ (http://www.rcsb.org/)..

‡ To whom correspondence may be addressed. Tel.: 41-61-3249252; Fax: 41-61-3247534; E-mail: gabriele.weitz@pharma.novartis.com or joerg.kallen@pharma.novartis.com.

[1] The abbreviations used are: LFA, lymphocyte function-associated antigen; I domain, inserted domain; ICAM, intercellular adhesion molecule; L-site, lovastatin site; mAb, monoclonal antibody; MIDAS, metal ion-dependent adhesion site; REMA, reporter epitope monitoring assay; RT, room temperature.

TABLE I
X-ray data collection and refinement statistics

	α_L I domain/LFA878	α_L I domain/LFA703
Crystal data		
Space group	$P2_12_12_1$	$P4_32_12$
Unit cell dimensions (Å)	$a = 71.9$; $b = 77.4$; $c = 92.3$	$a = b = 116.7$; $c = 82.7$
No. complexes/asymmetric unit	2	2
Intensity data processing		
Resolution (highest resolution bin) (Å)	8–2.1 (2.17–2.10)	8–2.2 (2.28–2.2)
R_{sym} (%)[a]	6.7 (23.6)	9.4 (28.6)
No. of measurements	123,226	213,739
No. of unique reflections	29,635	28,795
Completeness (%)	98.8 (99.8)	99.8 (100.0)
$\langle I/\sigma(I)\rangle$	22.5 (6.5)	22.7 (7.8)
Refinement statistics		
Resolution (highest resolution bin) (Å)	8–2.1 (2.15–2.10)	8–2.2 (2.25–2.20)
R_{cryst}/R_{free} (%)[b]	19.1/21.3 (23.3/27.7)	16.1/20.6 (18.2/27.3)
$\langle B\rangle$ for protein/ligand (Å^2)	34.3/43.1	34.2/37.4
Rmsd bond lengths (Å)[c]	0.014	0.018
Rmsd bond angles (°)[c]	1.38	1.51

[a] $R_{sym} = \Sigma|I - \langle I\rangle|/\Sigma I$, where I is observed intensity, and $\langle I\rangle$ is average intensity obtained from multiple observations of symmetry related reflections.
[b] $R_{cryst} = \Sigma\|F_{observed} - F_{calculated}\|/\Sigma F_{observed}$. R_{free} is R_{cryst}, calculated by using 5% of the data, chosen randomly, and omitted from refinement.
[c] Rmsd is root mean square deviation.

compounds via the L-site have been performed in assays involving the isolated I domain, purified LFA-1, or LFA-1 expressed on cell lines. Direct proof for L-site occupancy by lovastatin or statin derivatives in a more physiological setting is lacking.

Utilizing x-ray crystallography, we investigate here for the first time the molecular basis for improved LFA-1 inhibition by the previously described statin-based inhibitor LFA703 (12, 17) and the newly synthesized compound LFA878. Furthermore, we show that improved LFA-1 inhibition via the L-site can be detected *in vitro* in human blood and *ex vivo* in blood from treated animals. Our results in carrageenan-induced rat paw edema further substantiate the expectation that inhibitors targeting the L-site may have therapeutic potential as anti-inflammatory agents.

EXPERIMENTAL PROCEDURES

Crystallization and Structure Determination of the α_L I Domain/LFA878 Complex—For the α_L I domain, the construct comprising residues Lys^{127}–Gly^{311} was used, and purification was performed as reported previously (11). The complex α_L I domain/LFA878 was prepared by adding the ligand (100 mM solution in Me_2SO) to the protein solution (12.7 mg/ml 10 mM $MgSO_4$) in a 3:1 molar ratio. Crystals with maximal dimensions up to 0.4 mm could be grown by the hanging drop vapor diffusion method. Two microliters of α_L I domain/LFA878 were mixed with an equal volume of well solution (0.085 M sodium citrate, pH 5.6, 0.17 M ammonium acetate, 15% glycerol, and 25.5% (w/v) polyethylene glycol 4000) and allowed to equilibrate against 1 ml of the latter at 20 °C. Diffraction data were collected to 2.1 Å at 20 °C on a Mar345 imaging plate detector at the Swiss-Norwegian beamline of the European Synchrotron Facility (Grenoble, France). After data processing with the HKL software suite (19) and the CCP4-package (20), initial phases were obtained by molecular replacement with X-PLOR, Version 3.1 (21) using our coordinates of LFA-1 I domain/lovastatin (11) as a search model. Manual rebuilding was done with O (22) and refinement with REFMAC5 (23). Five percent of the unique data were randomly selected for the calculation of R_{free}. The two complexes in the asymmetric unit were refined without non-crystallographic restraints. The final refinement model includes two α_L I domains (residues Gly^{128}–Ile^{309}), two LFA878 ligands, two magnesium ions, 148 water molecules, and has good stereochemistry (overall G value = 0.20; see Table I for crystal data, data collection, and refinement statistics) (24).

Crystallization and Structure Determination of the αL I Domain/LFA703 Complex—The complex α_L I domain/LFA703 was prepared as for LFA878. Crystals with maximal dimensions up to 0.3 mm could be grown by the hanging drop vapor diffusion method. One microliter of α_L I domain/LFA703 was mixed with an equal volume of well solution (0.17 M ammonium acetate, pH 4.6, 0.085 M sodium acetate, 15% glycerol, and 26% (w/v) polyethylene glycol 4000) and allowed to equilibrate against 0.7 ml of the latter at 20 °C. Diffraction data were collected to 2.2 Å at 20 °C on a Mar345 imaging plate detector at the Swiss-Norwegian beamline of the European Synchrotron Facility (Grenoble, France). Data processing, rebuilding, and refinement were done as for LFA878. The final refinement model includes two α_L I domains (residues Gly^{128}–Ile^{309}), two LFA703 ligands, two magnesium ions, 278 water molecules, and has good stereochemistry (overall G value = 0.02; see Table I).

LFA-1 Binding Assays—The cell-free LFA-1/ICAM-1 binding assay quantifies the binding of biotinylated recombinant ICAM-1 to immobilized LFA-1. The HUT78/ICAM-1 adhesion assay quantifies the binding of fluorescently labeled HUT78 cells to immobilized recombinant ICAM-1. Both assays were performed as described previously (11).

Anti-LFA-1 mAbs Binding to Jurkat Cells—The effect of the compounds on the conformational status of LFA-1 was tested as described previously (17). Briefly, Jurkat cells were pre-incubated with the compounds at a final concentration of 50 μM in Tris-buffered saline containing 150 mM NaCl, 2 mM $MgCl_2$, 2 mM $MnCl_2$, and 0.5% bovine serum albumin, pH 7.4 (assay buffer) at room temperature (RT) for 20 min followed by the addition of the anti-LFA-1 mAbs. After 25 min at RT, cells were washed two times with assay buffer and counterstained with Alexa Fluor® 488 goat anti-mouse IgG (H+L) conjugate (Molecular Probes, Leiden, Netherlands) diluted 1:175 in assay buffer for 30 min at RT. After a washing step, antibody binding was immediately analyzed by flow cytometry on a FACScan (BD Biosciences). Mean fluorescence intensities (geometric mean) were calculated using the CellQuest software. Mean fluorescence intensities were corrected for background staining by subtracting the mean fluorescent intensity of the appropriate isotype-matched negative controls. Mean fluorescence intensities of the solvent controls were set as 100%. Inhibition of anti-LFA-1 mAb binding induced by inhibitor treatment was expressed as a percentage of these controls.

Whole Blood LFA-1 Reporter Epitope Monitoring Assay (LFA-1 REMA)—The LFA-1 inhibitors were dissolved and diluted in Me_2SO. Heparinized human blood samples or blood samples from different animal species (198 μl) were mixed with the compound solution or Me_2SO (2 μl) and incubated for 25 min at RT. The compound containing blood samples (90 μl) were then transferred to 96-well microtiter plates. The fluorescein isothiocyanate-conjugated mAb R7.1 (BioSource, Camarillo, CA) and the isotype control mAb were diluted in phosphate-buffered saline, and 10 μl was added to the samples (final concentration was 2–3 μg of mAb per milliliter of blood). After 25 min at RT, the blood samples (100 μl) were transferred to tubes containing 1 ml of FACS lysing solution (BD Biosciences), mixed, and incubated for 10 min in the dark at RT. Then the samples were centrifuged at 200 × g for 5 min. The supernatants were removed, and the pellets were washed two times in 1 ml of Tris-buffered saline (pH 7.4) containing 0.5% bovine serum albumin and then resuspended in 150 μl of the same buffer. Bound antibody was detected by flow cytometry gating the major leukocyte subpopulations according to their light scatter properties. In each sample, 20,000 lymphocytes were counted. In control experiments, unlabeled mAb TS2/4 was diluted and added to the blood samples (final concentration was 2.5 μg of mAb per milliliter of blood). After lysis and washing steps the Alexa Fluor® 488 goat anti-mouse IgG conjugate

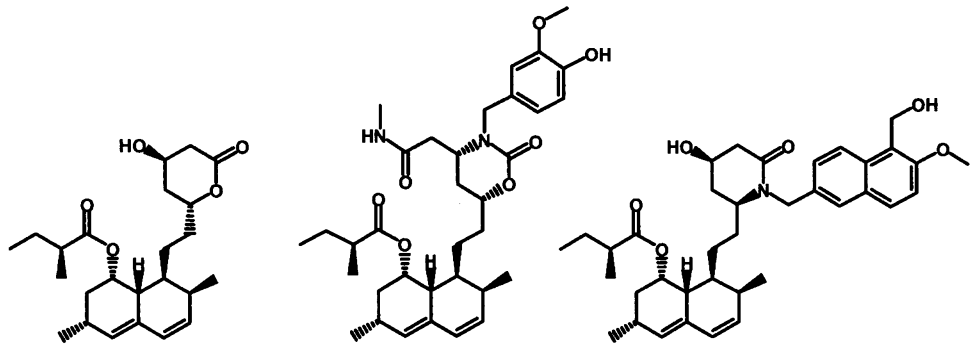

FIG. 1. **Chemical structures of the low molecular weight LFA-1 inhibitors lovastatin, LFA703, and LFA878 and their activities in LFA-1 dependent binding assays.** The activities of the compounds were determined by a cell-free, enzyme-linked immunosorbent assay (ELISA)-type LFA-1/ICAM-1 binding assay (*LFA-1*) and the HUT78/ICAM-1 adhesion assay (*HUT78*) as described under "Experimental Procedures." Mean values ± S.D. of at least three independent experiments are shown.

diluted 1:150 in Tris-buffered saline, pH 7.4, containing 0.5% bovine serum albumin was added. The samples were incubated for 30 min, and bound mAb TS2/4 was quantified by flow cytometry as described.

Ex Vivo Rabbit LFA-1 REMA—Female Russian dwarf rabbits received 0.1 ml/kg Prequillan (10 mg/ml) subcutaneously. Compounds dissolved in a mixture of cremophor EL and ethanol (2:1) (w/w) and then diluted further with 5% glucose (1:3) (v/v) were administered intravenously by bolus injection (right ear; 1.5 ml per rabbit). Blood samples (200 μl) were taken from the left ear at indicated time points and placed into microtubes containing heparin. The blood samples were stored on ice until analysis. Ninety microliters of each sample were transferred to microtiter plates, and REMA analysis was performed as described above. Baseline values were determined in blood samples taken 15 min before compound administration. The animal experiments were conducted in accordance with the animal experimentation guidelines and laws laid down by the Swiss Federal and Cantonal Authorities.

Carrageenan-induced Paw Edema in Rats—Male OFA rats were treated orally with LFA878 (3, 10, and 30 mg/kg), diclofenac (3 mg/kg), or the respective vehicle controls (vehicle for LFA878 was a mixture of cremophor EL and ethanol (2:1) (w/w) diluted 1:3 (v/v) with 5% glucose; vehicle for diclofenac was Tween 80/0.75% methylcellulose). The anti-LFA-1 mAb WT.1 (NatuTec, Frankfurt, Germany) was diluted in phosphate-buffered saline and administered at a concentration of 2.5 mg/kg. One hour later the rats received a 100-μl intra-plantar injection of a 1% (w/v) carrageenan solution in 0.9% saline in the hind paw, and the volume of the paw was measured by plethysmography. The paw volume measurements were repeated at 3 and 5 h after injection of the carrageenan. Percentage inhibition of paw swelling at 3 and 5 h was calculated by reference to vehicle-treated animals (0% inhibition). The animal experiments were conducted according to the animal experimentation guidelines and laws laid down by the Swiss Federal and Cantonal Authorities.

RESULTS

X-ray Structures of the Complexes α_L I Domain/LFA703 and α_L I Domain/LFA878 Identify Novel Subpockets within the L-site—The compounds LFA703 and LFA878 are two examples of a series of lovastatin-derived inhibitors that inhibit LFA-1 function more potently than lovastatin itself (Fig. 1). Both compounds blocked LFA-1 mediated binding to ICAM-1 with IC_{50} values in the low nanomolar range in cell-free and cell-based *in vitro* assays, whereas lovastatin was only active in the micromolar range (Fig. 1). To determine the structural basis for this improved activity, we solved the crystal structures of the I domain portion of LFA-1 bound to LFA703 or LFA878 at resolution limits of 2.2 and 2.1 Å, respectively (Fig. 2). The crystal form for LFA878 is very similar to the one reported previously for lovastatin (with a local dyad relating the two complexes in the asymmetric unit) (11), whereas the form for LFA703 is new and different (no local dyad relating the two complexes). Interestingly, for LFA703 the C-terminal residues of the I domain monomers form parallel β-sheet interactions with the respective residues from a neighboring molecule, in contrast to the antiparallel β-sheet interactions in the LFA878 or lovastatin complexes. This finding demonstrates the structural adaptability of the linker region after the helix α_7 and suggests possible structural changes occurring upon the activation of LFA-1. Moreover, a new type of interaction with the MIDAS site is observed in the crystal form for LFA703. The Mg^{2+} in the MIDAS itself is coordinated in an identical way as that seen for the other α_L I domain/statin-based inhibitor complexes or the uncomplexed α_L I domain (25). In all the latter cases (including the complex with LFA703) the I domain is in its low affinity form, which is characterized (among other features) by a direct coordination of Mg^{2+} by Asp^{239}. The direct coordination is thought to reduce the electrophilicity of Mg^{2+} and, thus, to weaken the interaction with Glu^{34} of ICAM-1 (3). This hypothesis is now corroborated with the new tetragonal crystal form of the α_L I domain/LFA703 complex, which does not show a direct interaction but only a water-mediated, indirect interaction between the Mg^{2+} (protomer B) and a glutamate residue (Glu^{218}) from a neighboring protomer A (Fig. 2*F*).

Both LFA703 and LFA878 were found to bind to the L-site of the α_L I domain (Fig. 2, *A* and *B*) and displayed a clear difference electron density before, present in the models (Fig. 2, *C* and *D*). The decalin moieties of the statin derivatives adopt very similar positions within the respective x-ray structures even though different interactions between the I domain monomers occur at the carboxyl termini of the different crystal forms (Fig. 2*E*). The main contacts between LFA703 and the L-site (distance cutoff of 4.2 Å between non-hydrogen atoms) are mediated by the residues Gly^{128}, Val^{130}, Leu^{132}, Phe^{153}, Tyr^{166}, Thr^{231}, Val^{233}, Ile^{235}, Ile^{255}, Tyr^{257}, Glu^{284}, Phe^{285}, Lys^{287}, Leu^{298}, Glu^{301}, Leu^{302}, Lys^{305}, and Ile^{306}. Interestingly, the carbonyl oxygen of the isobutyl-ester moiety attached to the decalin ring of LFA703 contributes a water-mediated hydrogen bond to both NZ-Lys^{287} and OE1- or OE2-Glu^{284}. The substituted naphthyl of LFA703 adopts

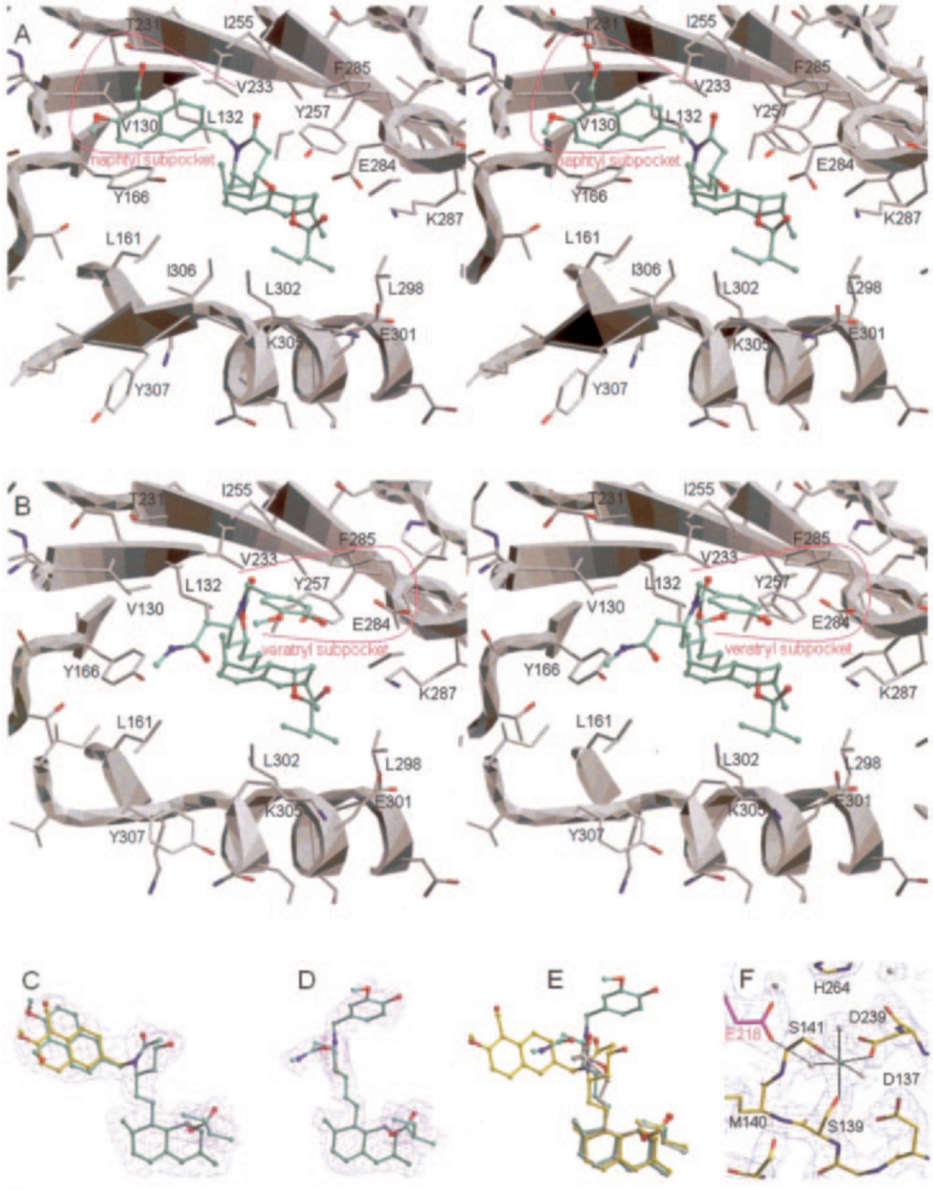

FIG. 2. **X-ray structures of the complexes α_L I domain/LFA703 and α_L I domain/LFA878.** *A*, stereo image of the L-site for α_L I domain/LFA703. I domain residues and ribbon representation are in *white*, LFA703 in *cyan* (oxygens are *red*, and nitrogens are *blue*). The substituted naphthyl group of LFA703 occupies a region (the naphthyl subpocket, colored *magenta*) formed mainly by Val^{130}, Thr^{231}, Val^{233}, and Ile^{255}. *B*, stereo image of the L-site for α_L I domain/LFA878 (coloring as for LFA703). The veratryl group of LFA878 occupies a region (the veratryl-subpocket, colored *magenta*) formed mainly by Tyr^{257}, Glu^{284}, and Phe^{285}. A comparison with the I domain/LFA703 complex shows that Glu^{284} has dramatically changed its side-chain conformation. *C*, $F_o - F_c$ electron density (contour level 3σ, 8–2.2 Å) before LFA703 was inserted into the model. Superposed is the final model of LFA703 (carbons are *cyan/yellow*, oxygens are *red*, and nitrogens are *blue*). The naphthyl group adopts two alternate conformations. *D*, $F_o - F_c$ electron density (contour level 3σ, 8–2.1 Å) before LFA878 was inserted into the model. Superposed is the final model of LFA878 (coloring as for LFA703). *E*, superposition of LFA703 (carbons are *yellow*), LFA878 (carbons are *cyan*), and lovastatin (carbons are *white*) using Cα atoms of the respective α_L I domains. The decalin moieties occupy practically identical positions. *F*, MIDAS site for α_L I domain/LFA703. Final $2F_o - F_c$ electron density (contour level 3σ, 8–2.2 Å) is shown in *blue*; carbons are *yellow*, oxygens are *red*, nitrogens are *blue*, water molecules are *white*, and the Mg^{2+} ion is *cyan*. Selected hydrogen bonds are shown as *black lines* (*dashed lines* for the interaction with neighboring molecule). Because of the direct coordination by Asp^{239}, the electrophilicity of Mg^{2+} is reduced so that a glutamate (Glu^{218}, colored *magenta*) from a neighboring molecule is only interacting indirectly (via a water molecule) with the Mg^{2+} in the MIDAS site. Single letter amino acid abbreviations are used with position numbers throughout the figure.

two alternate conformations (for which the naphthyl groups are in the same plane), allowing the hydroxy-methylene group of the naphthyl in one conformation to form a hydrogen bond with OG1-Thr^{231} (Fig. 2, *A* and *C*). This region within the L-site is not reached by LFA878 or lovastatin and constitutes a new L-site subpocket, designated here the "naphthyl subpocket," formed mainly by the side chains of Val^{130}, Thr^{231}, Val^{233}, and Ile^{255}. A least squares superposition of the α_L I domains in the complexes with LFA703 and lovastatin shows that the protein backbones are similar (*e.g.* the root mean squares deviation for the Cα-atoms of residues Gly^{128}–Lys^{304} from the respective protomers A is 0.36 Å, and from the respective protomers B it is 0.52 Å) but display significant changes at the carboxyl-terminal residues Lys^{305}–Ile^{309}, which are involved in different types of interactions with neighboring molecules (parallel and antiparallel β-sheet interactions, respectively).

The main contacts between LFA878 and the L-site (distance cutoff of 4.2 Å between non-hydrogen atoms) are mediated by the residues Leu^{132}, Phe^{153}, Val^{233}, Ile^{235}, Ile^{255}, Tyr^{257}, Glu^{284}, Phe^{285}, Lys^{287}, Leu^{298}, Glu^{301}, Leu^{302}, and Lys^{305}. Clear structural differences compared with LFA703 and lovastatin occur for the veratryl part of LFA878. The terminal veratryl group of LFA878 occupies a region of the L-site not utilized by the chemical groups of lovastatin or LFA703. This region, designated here the "veratryl subpocket," is formed mainly by the side chains of Tyr^{257}, Glu^{284}, and Phe^{285}. The veratryl group is tilted toward the carboxylate group of Glu^{284}, thereby enabling

TABLE II
Effect of LFA878 on the binding of different mAbs to LFA-1 expressed on Jurkat cells

Jurkat cells were incubated with the indicated mAbs in the presence of 50 μM LFA878 and 2 mM Mn^{2+}/Mg^{2+}. Bound antibody was quantified by flow cytometry as described under "Experimental Procedures." Compound-induced inhibition of mAb binding to LFA-1 is expressed as percentage of solvent control. Each value represents the mean ± S.D. of three independent experiments.

mAb	Epitope	Inhibition of antibody binding to Jurkat cell LFA-1
		%
TS1/22	α_L I domain	4.5 ± 9.0
25.3.1	α_L I domain	12.5 ± 19
R7.1	α_L I domain	96.4 ± 6.16
Clone 38	α_L I domain	5.4 ± 7.9
TS2/4	α_L β propeller	−6.3 ± 12.4
IB4	β_2 I-like domain	5.7 ± 15.4
R3.3	β_2 I-like domain	1.8 ± 16.8

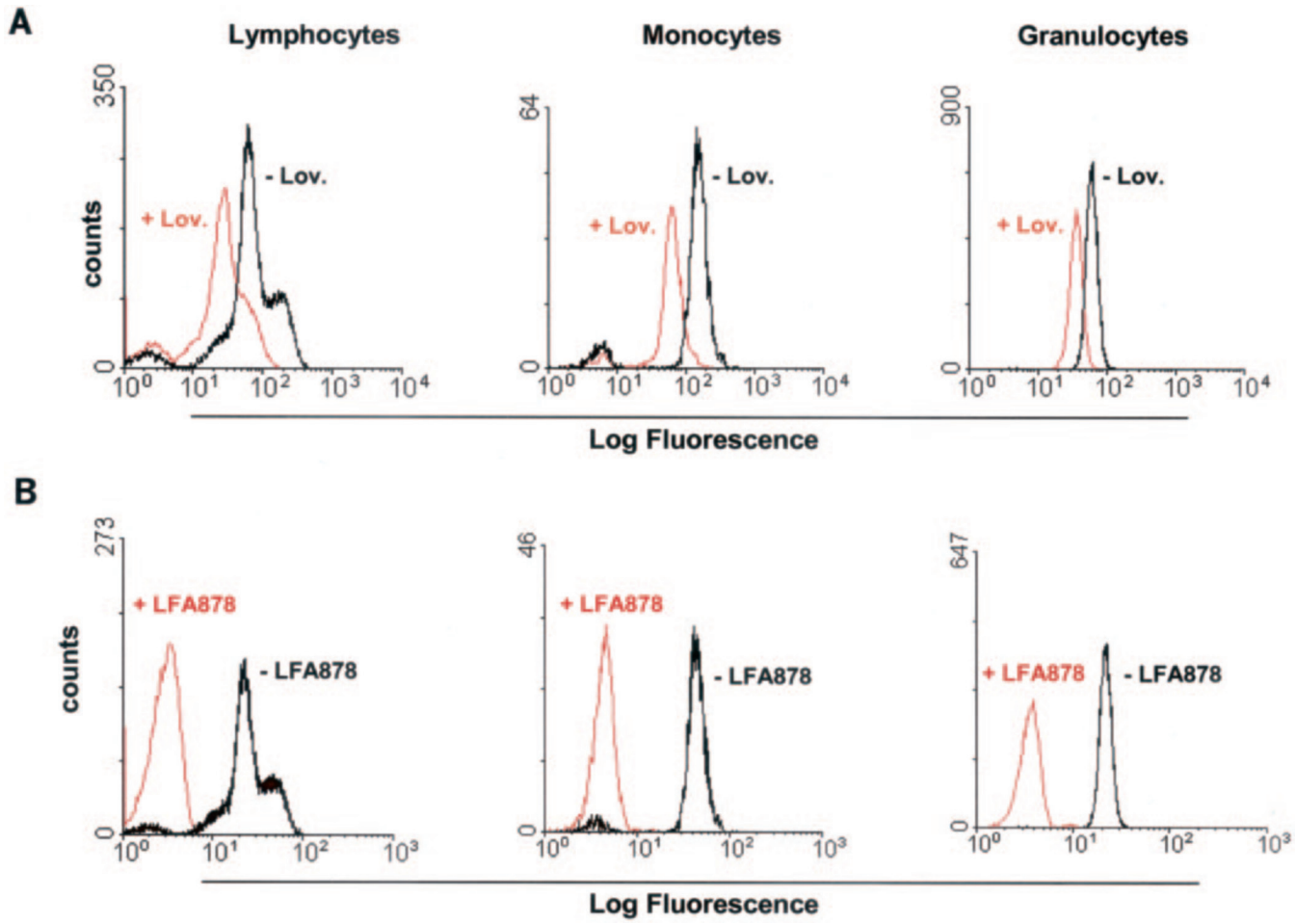

FIG. 3. **Lovastatin and LFA878 inhibit the binding of mAb R7.1 to LFA-1 in human blood *in vitro*.** The binding of fluorescein isothiocyanate-labeled mAb R7.1 to leukocytes in human whole blood was quantified in the presence of lovastatin (*Lov.*) (100 μM) (*A*) or LFA878 (30 μM) (*B*) by flow cytometry as described under "Experimental Procedures." *Red profiles* indicate the binding of mAb R7.1 to lymphocytes, granulocytes, or monocytes in the presence of compound; *black profiles* such binding in the presence of the solvent control. A representative experiment is shown.

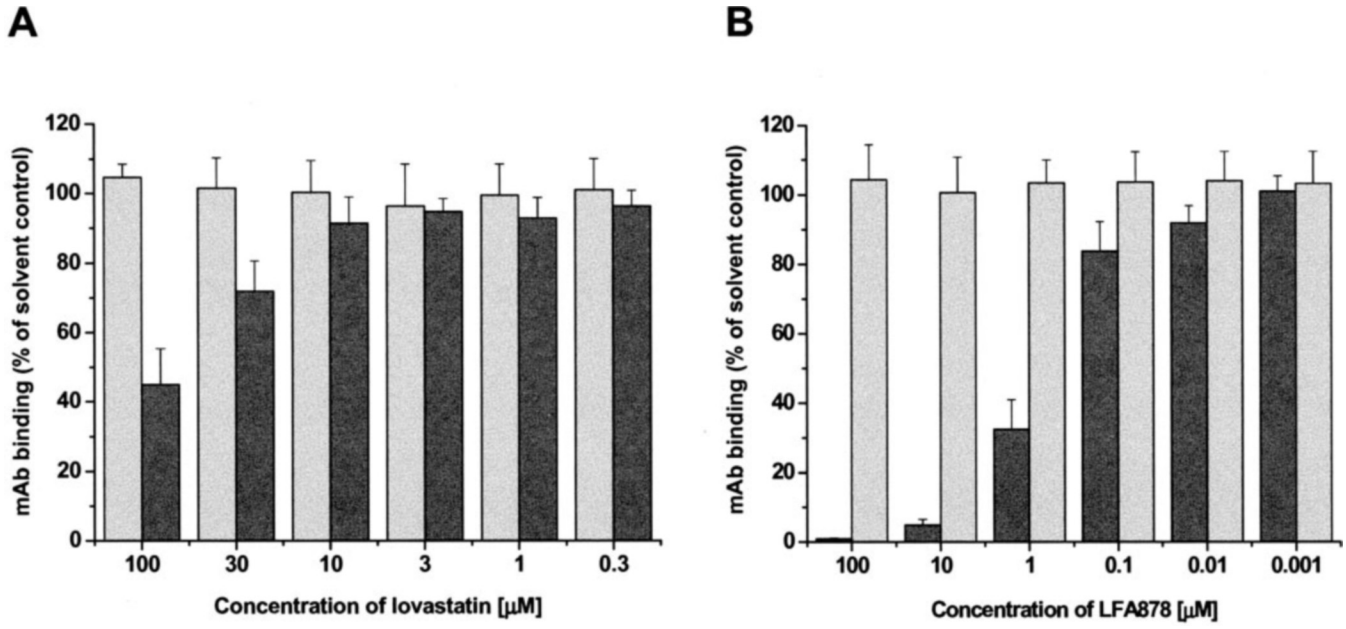

FIG. 4. **Effect of lovastatin and LFA878 on mAb R7.1 and mAb TS2/4 binding to LFA-1 in human blood *in vitro*.** The binding of the mAb R7.1 (*gray bars*) and mAb TS2/4 (*light gray bars*) to LFA-1 in human whole blood was quantified by flow cytometry in the presence of lovastatin (*A*) or LFA878 (*B*) as described under "Experimental Procedures." Each bar represents the mean value ± S.D. calculated from the separate analyses of the major leukocyte subsets. A representative experiment of three independent experiments is shown.

a hydrogen bond between the *p*-hydroxy group and Glu^{284} (Fig. 2*B*). This hydrogen bond formation also modifies the side-chain conformation of Glu^{284} dramatically (shift by ~3 Å), as compared with the I domain/lovastatin and the LFA703 complexes (Fig. 2, *A* and *B*). The methyl-amide group attached to the carbamate ring of LFA878 does not show well defined electron density and is thus flexible. A least squares superposition of the α_L I domains in the complexes with LFA878 and lovastatin shows that, apart from the side-chain difference of Glu^{284}, the protein moieties in general have not changed significantly (*e.g.* the root means square deviation for the Cα atoms of residues Gly^{128}–Ile^{309} from the respective protomers A is 0.18 Å, and from the respective protomers B it is 0.24 Å).

In summary, the structural analysis of the I domain/LFA703 and I domain/LFA878 complexes identified two novel subpockets within the L-site that were not yet occupied by chemical groups of lovastatin. Moreover, our data indicate that occupancy of these new L-site subpockets leads to increased LFA-1 inhibition *in vitro* (Figs. 1 and 2). The *in vitro* activities of the statin-derived compounds further suggest that the engagement of the "veratryl subpocket" is the relatively more efficient way to block LFA-1.

Occupancy of Different L-site Subpockets Leads to Distinct Epitope Changes in LFA-1—As reported previously, engagement of the L-site by statins or statin-derived LFA-1 inhibitors induces distinct epitope changes in cation-activated LFA-1 (17). Some of the inhibitors affected epitopes on the α_L I domain but not on the β_2 I-like domain of LFA-1, whereas other inhibitors including LFA703 and lovastatin were able to modify epitopes on both domains (17). LFA878 was found to only affect the α I domain (Table II). The compound induced an almost complete loss of the mAb R7.1 epitope on the α_L I domain, whereas other epitopes assessed on the α_L I domain and β_2 I-like domain remained largely unchanged (Table II). Based on the crystal structures described above, the differential effects of LFA878 and LFA703 on the conformational state of LFA-1 were not entirely unexpected. Our data suggest that occupancy of the veratryl subpocket does not affect the conformational state of the β_2 I-like domain of LFA-1, in contrast to the occupancy of the naphthyl subpocket.

Inhibitor-induced LFA-1 Epitope Changes Can Be Measured in Vitro in Human Blood—Lovastatin and the more potent statin-derived LFA-1 inhibitor LFA878 were selected to confirm L-site occupancy and improved LFA-1 inhibition under more physiological conditions in whole blood. For this purpose, we established a flow cytometry assay that allows us to measure the degree of epitope changes on the α_L I domain as an indicator for L-site occupancy in blood. Based on the fact that all of the statin compounds investigated so far were able to induce the loss of the mAb R7.1 epitope, we used this epitope as the reporter epitope for the assay. The LFA-1 REMA was applied to blood samples from healthy volunteers. We found that both compounds reduced the binding of the mAb R7.1 to LFA-1 in whole blood (Fig. 3, *A* and *B*). Furthermore, we showed that the inhibition of mAb R7.1 binding by the compounds occurred in a concentration-dependent manner, whereas the interaction of the anti-LFA-1 mAb TS2/4 with LFA-1 was not affected in the blood samples (Fig. 4). Importantly, the activity of lovastatin and LFA878 in blood as assessed by the REMA correlated well with the inhibitory activity of the compounds determined in the HUT78 cell/ICAM-1 adhesion assay (Figs. 1 and 4). This finding indicates that the degree of the mAb R7.1 epitope loss reflects the inhibitory potential of the compounds. Taken together, these data suggest that it may be feasible to quantify allosteric inhibition of LFA-1 via the L-site *ex vivo* in blood samples from treated animals or patients.

TABLE III
Effect of lovastatin and LFA878 on mAb R7.1 binding in whole blood in vitro

The binding of fluorescein isothiocyanate-labeled mAb R7.1 to leukocytes in blood samples from healthy volunteers and different animal species was quantified in the presence of lovastatin or LFA878 as described under "Experimental Procedures." Mean values ± S.D. of at least three independent experiments are shown. n.d., not determined.

Whole blood samples	Inhibition of mAb R7.1 binding by lovastatin	Inhibition of mAb R7.1 binding by LFA878 (IC_{50})
	%	μM
Human	10 ± 2.6[a] 59 ± 4.5[b]	0.3 ± 0.09
Rabbit	5.3 ± 2.6[a] 18 ± 3.2[b]	0.3 ± 0.2
Dog	n.d.	3.0 ± 1.0
Rhesus monkey	n.d.	1.4 ± 0.56
Cynomolgus monkey	n.d.	3.2 ± 0.7

[a] At 10 μM.
[b] At 100 μM.

Inhibitor-induced LFA-1 Epitope Change Is Detectable in Vitro in Blood from Different Animal Species—To establish the concept of monitoring L-site engagement in treated animals, we applied the REMA to blood samples from different animal species including mice, rats, rabbits, dogs, and monkeys. The LFA-1 REMA was not applicable to blood samples from rodents because of the lack of mAb R7.1 cross-reactivity (not shown). In contrast, the mAb R7.1 cross-reacted with rabbit, dog, and monkey LFA-1, allowing the application of the LFA-1 REMA to blood samples from these animal species. We found that LFA878 prevented the binding of mAb R7.1 to rabbit LFA-1 with the same potency as the binding to human LFA-1 in whole blood (Table III). Higher compound concentrations were required to detect mAb R7.1 epitope change in dog and monkey blood samples (Table III). Lovastatin was found to be weakly active in rabbit blood samples (Table III). These results indicate that rabbits are the best suited animal species for demonstrating L-site engagement by statin-derived compounds *ex vivo*.

Inhibitor-induced Epitope Change Is Detectable ex Vivo in Blood Samples from Treated Rabbits—Rabbits were treated intravenously with 4 mg/kg lovastatin or LFA878. For REMA analysis, blood samples were drawn at different time points after administration. We found that LFA878 was able to prevent the binding of mAb R7.1 to rabbit LFA-1 by >90% compared with baseline values for up to 1 h post-dose (Fig. 5). Thereafter, inhibition decreased and binding of mAb R7.1 returned close to baseline (Fig. 5). Based on these REMA results and the LFA878 blood concentrations determined by liquid chromatography-mass spectroscopy analysis (data not shown), the activity of the LFA-1 inhibitor in rabbits was calculated. We found that the compound inhibited mAb R7.1 binding *ex vivo* with an IC_{50} of 0.323 ± 0.158 (n = 3). This value correlated well with the REMA IC_{50} value determined *in vitro* and the inhibitory activity of LFA878 measured in the HUT78/ICAM-1 adhesion assay.

Although lovastatin was found to be a weak inhibitor of human and rabbit LFA-1 *in vitro*, the statin was included in the rabbit study. We were able to detect inhibition of mAb R7.1 binding to LFA-1 shortly after intravenous application of the compound (Fig. 5). This inhibition was achieved at lovastatin blood concentrations of 18 μM (data not shown). However, 30 min after administration, the binding of the mAb R7.1 was comparable with baseline values reflecting the rapid clearance of lovastatin from the circulation (Fig. 5). This result indicates

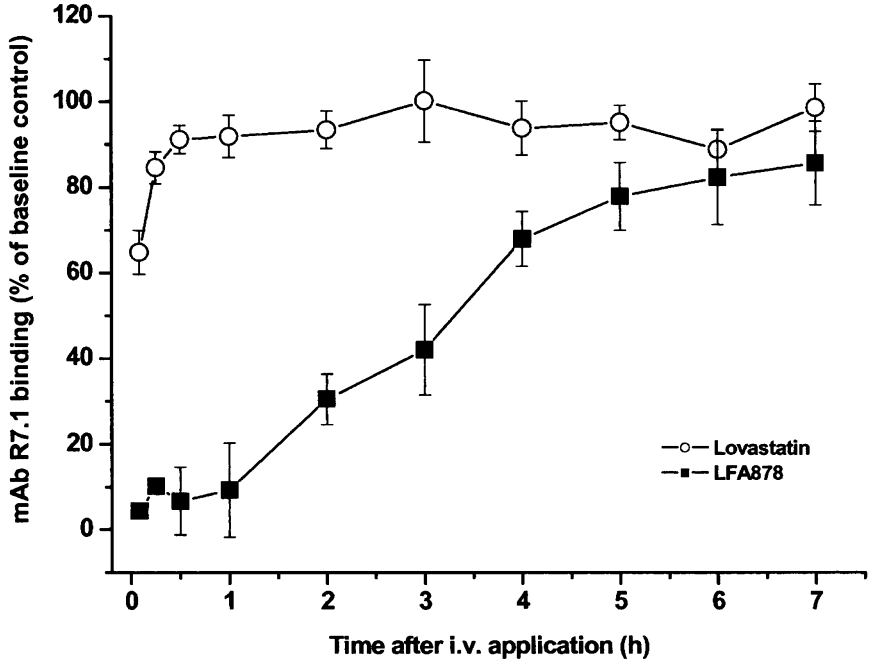

FIG. 5. ***Ex vivo*** **analysis of blood samples from rabbits treated with lovastatin or LFA878.** Rabbits were treated intravenously (*i.v.*) with 4 mg/kg lovastatin or LFA878. Blood samples were taken at indicated time points postdosing and analyzed for mAb R7.1 binding to LFA-1 as described under "Experimental Procedures." Baseline values were determined 15 min before compound administration and set as 100%. A representative experiment of three independent experiments is shown.

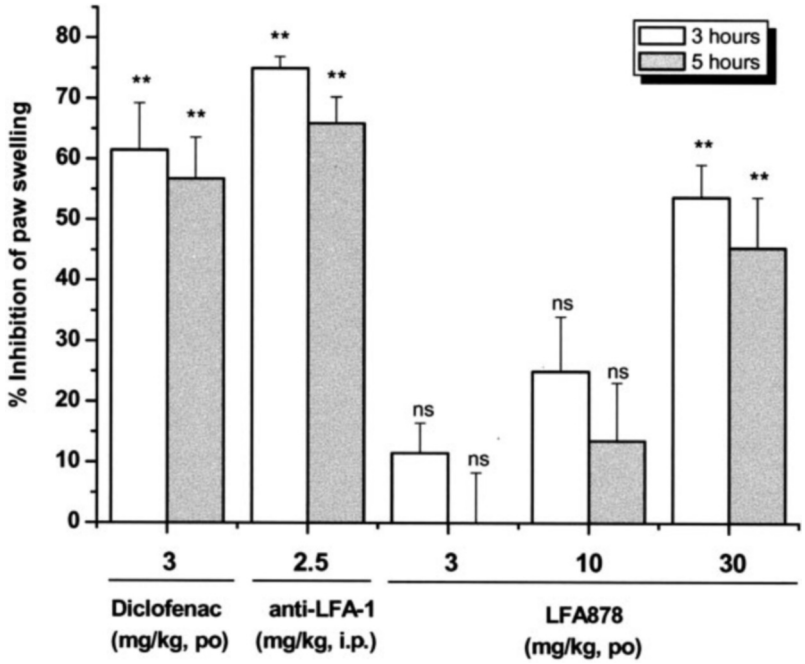

FIG. 6. **Effect of LFA878 carrageenan-induced rat paw edema.** Paw edema was induced in rats by an intraplantar injection of carrageenan. Paw diameters were measured at the time of carrageenan injection (0 h) and at 3 and 5 h post-injection as described under "Experimental Procedures." Compounds were administered 1 h before the carrageenan injection. LFA878 was dosed orally (*po*) at 3, 10, and 30 mg/kg and diclofenac at 3 mg/kg. The anti-LFA-1 mAb WT.1 was given intraperitoneally (i.p.) at 2.5 mg/kg. Columns represent means ± S.E. with $n = 6$; **, $p < 0.01$; *ns*, not significant. Analysis of variance assay plus Dunnett's test *post hoc. i.v.*, intravenously.

for the first time that a cholesterol-lowering agent is able to interact with LFA-1 *in vivo*. Moreover, the comparison of lovastatin and LFA878 in this rabbit study further establishes LFA878 as a statin-derived compound optimized for LFA-1 inhibition.

LFA878 Inhibits the Inflammatory Response in the Rat Carrageenan Paw Edema Model—We used the carrageenan-induced edema rat model to investigate the anti-inflammatory effect of the novel LFA-1 inhibitor LFA878. The compound produced a dose-dependent anti-inflammatory effect in this model after oral administration with the maximal dose of 30 mg/kg, resulting in 54 and 45% inhibition 3 and 5 h after administration, respectively. The anti-rat LFA-1 mAb WT.1, given intraperitoneally, inhibited paw swelling by 75 and 66% at 3 and 5 h (Fig. 6). Control IgG had no effect when applied under same conditions (data not shown). The anti-inflammatory drug diclofenac (included as a positive drug control) at 3 mg/kg also showed a marked inhibition at both 3 and 5 h in this model. These data are not only the first that demonstrate the LFA-1 dependence of the rat carrageenan paw edema model but also confirm that L-site engagement by a statin-derived compound results in anti-inflammatory effects *in vivo*.

DISCUSSION

In this report we describe two new distinct subpockets within the allosteric L-site of LFA-1 termed naphthyl subpocket and veratryl subpocket. Occupancy of these subpockets was found to be associated with increased LFA-1 inhibition, indicating that both subpockets are important for LFA-1 activation and function. The biological relevance of the naphthyl subpocket is further supported by our previous observation that the replacement of the L-site residue Val^{130} (which constitutes a part of

the naphthyl subpocket) by tryptophan completely abrogates LFA-1-mediated adhesion to ICAM-1 (12).

Interestingly, occupancy of the L-site subpockets by the inhibitory compounds resulted in differential effects on the LFA-1 subunits as monitored by conformation-sensitive mAbs. LFA878 binding led to epitope changes on the I domain of the α_L subunit but not on the I-like domain of the β_2 subunit, whereas binding of LFA703 affected both domains (17). The latter effect by LFA703 suggests that occupancy of the naphthyl subpocket triggers conformational alterations within LFA-1 that affect the interface formed between the two domains. Whether conformational changes of the I-like domain induced by inhibitors such as LFA703 have functional consequences distinct from LFA878-type inhibitors (beyond the degree of LFA-1 inhibition) remains to be investigated. LFA703 shares the prominent effect on the β_2 I-like domain with the recently described α/β I-like allosteric inhibitors (17). We propose that LFA703 belongs to a class of "hybrid" inhibitors that exhibit properties of α I allosteric and α/β I-like allosteric inhibitors.

Moreover, the fact that L-site engagement and, thus, the inhibition of LFA-1 by statin compounds can be detected in undiluted human blood substantiates the role of the L-site under physiological conditions. Furthermore, our studies utilizing whole blood from different animal species indicate that the allosteric L-site identified is conserved and can be engaged by low molecular weight inhibitors. Recent data by Woska *et al.* showing LFA-1 occupancy by α I allosteric inhibitors of the hydantoin class in human whole blood and blood from monkeys support our conclusions (26).

The investigations described here allowed us to also shed further light on the molecular mechanisms leading to anti-inflammatory effects of statins that are unrelated to their cholesterol-lowering activity (27, 28). It has been debated recently whether these anti-inflammatory properties of statins can be attributed, at least in part, to their effect on LFA-1 (29–32). We found that lovastatin is indeed able to bind to LFA-1 *in vivo*, at least at micromolar levels. However, our data do not allow us to answer the question of whether such binding occurs at lower nanomolar blood levels of statins in the therapeutic setting. In conclusion, our results suggest that compounds utilizing the newly described L-site subpockets may ultimately lead to orally available anti-inflammatory drugs of improved therapeutic benefit.

Acknowledgments—We thank Simone Schmutz, Bernhard Jost, and Christian Beerli for their excellent technical support, Wilfried Bauer for the synthesis of LFA878, and Dr. Sylvain Cottens for the synthesis of LFA703. We also thank Dr. Paul Ramage, Rene Hemmig, and Bernard Mathis for the purification of the LFA-1 I domain, the staff of the Swiss-Norwegian beam line at the European Synchrotron Radiation Facility for help during data collection, and Dr. T. Springer, Harvard Medical School, and Dr. A.-G. Schmidt for the critical review of the manuscript.

REFERENCES

1. Springer, T. A. (1994) *Cell* **76,** 301–314
2. Huang, C., Lu, C. & Springer, T. A. (1997) *Proc. Natl. Acad. Sci. U. S. A.* **94,** 3156–3161
3. Shimaoka, M., Xiao, T., Liu, J. H., Yang, Y., Dong, Y., Jun, C. D., McCormack, A., Zhang, R., Joachimiak, A., Takagi, J., Wang, J. H. & Springer, T. A. (2003) *Cell* **112,** 99–111
4. Lu, C, Shimaoka, M., Zang, Q., Takagi, J. & Springer, T. A. (2001) *Proc. Natl. Acad. Sci. U. S. A.* **98,** 2393–2398
5. Yang, W., Shimaoka, M., Chen, J. & Springer, T. A. (2004) *Proc. Natl. Acad. Sci. U. S. A.* **101,** 2333–2338
6. Grakoui, A., Bromley, S. K., Sumen, C., Davis, M. M., Shaw, A. S., Allen, P. M. & Dustin, M. L. (1999) *Science* **285,** 221–227
7. Cavazzana-Calvo, M., Bordigoni, P., Michel, G., Esperou, H., Souillet, G., Leblanc, T., Stephan, J. L., Vannier J. P., Mechinaud, F., Reiffers J., Vilmer, E., Landman-Parker, J., Benkerrou, M., Baruchel, A., Pico, J., Bernaudin, F., Bergeron, C., Plouvier, E., Thomas, C., Wijdenes, J., Lacour, B., Blanche, S. & Fischer, A. (1996) *Br. J. Haematol.*, **93,** 131–138
8. Hourmant, M., Bedrossian, J., Durand, D., Lebranchu, Y., Renoult, E., Caudrelier P., Buffet, R. & Soulillou, J. P. (1996) *Transplantation* **62,** 1565–1570
9. Lebwohl, M., Tyring, S. K., Hamilton, T. K., Toth, D., Glazer, S., Tawfik, N. H., Walicke, P., Dummer, W., Wang, X., Garovoy, M. R. & Pariser, D. (2003) *N. Engl. J. Med.* **349,** 2004–2013
10. Shimaoka, M. & Springer, T. A. (2003) *Nat. Rev. Drug. Discov.* **2,** 703–716
11. Kallen, J., Welzenbach, K., Ramage, P., Geyl, D., Kriwacki, R., Legge, G., Cottens, S., Weitz-Schmidt, G. & Hommel, U. (1999) *J. Mol. Biol.* **292,** 1–9
12. Weitz-Schmidt, G., Welzenbach, K., Brinkmann, V., Kamata, T., Kallen, J., Bruns, C., Cottens, S., Takada, Y. & Hommel, U. (2001) *Nat. Med.* **7,** 687–692
13. Liu, G., Link, J. T., Pei, Z., Reilly, E. B., Leitza, S., Nguyen, B., Marsh, K. C., Okasinski, G. F., von Geldern T. W., Ormes, M., Fowler, K. & Gallatin, M. (2000) *J. Med. Chem.* **43,** 4025–4040
14. Last-Barney, K., Davidson, W., Cardozo, M., Frye, L. L., Grygon, C. A., Hopkins, J. L., Jeanfavre, D. D., Pav, S., Qian, C., Stevenson, J. M. Tong, L., Zindell, R. & Kelly, T. A. (2001) *J. Am. Chem. Soc.* **123,** 5643–5650
15. Wattanasin, S., Albert, R., Ehrhardt, C., Roche, D., Sabio, M., Hommel, U., Welzenbach, K. & Weitz-Schmidt, G. (2003) *Bioorg. Med. Chem. Lett.* **13,** 499–502
16. Crump, M. P., Ceska, T. A, Spyracopoulos, L., Henry, A., Archibald, S. C., Alexander, R., Taylor, R. J., Findlow, S. C., O'Connell, J., Robinson, M. K. & Shock, A. (2004) *Biochemistry* **43,** 2394–2404
17. Welzenbach, K., Hommel, U. & Weitz-Schmidt, G. (2002) *J. Biol. Chem.* **277,** 10590–10598
18. Shimaoka, M., Salas, A, Yang, W., Weitz-Schmidt, G. & Springer, T. A. (2003) *Immunity* **19,** 391–402
19. Otwinowski, Z. & Minor, W. (1997) *Methods Enzymol.* **276,** 307–326
20. Collaborative Computational Project No. 4 (1994) *Acta Crystallogr. Sect. D Biol. Crystallogr.* **50,** 760–763
21. Bruenger, A. T. (1992). *X-PLOR Version 3.1: A System for X-ray Crystallography and NMR*, Yale University Press, New Haven, CT
22. Jones, T. A., Zou, J.-Y., Cowan, S. W. & Kjeldgaard, M. (1991) *Acta Crystallogr. Sect. A* **47,** 110–119
23. Murshudov, G. N., Vagin, A. A. & Dodson, E. J. (1997) *Acta Crystallogr. Sect. D Biol. Crystallogr.* **53,** 240–255
24. Laskowski, R. A., MacArthur, M. W., Moss, D. S. & Thornton, J. M. (1993) *J. Appl. Crystallogr.* **26,** 283–291
25. Qu A. & Leahy D. J. (1995) *Proc. Natl. Acad. Sci. U. S. A.* **92,** 10277–10281
26. Woska J. R., Jr., Last-Barney K., Rothlein R., Kroe R. R., Reilly P. L., Jeanfavre, D. D., Mainolfi, E. A., Kelly, T. A., Caviness, G. O., Fogal, S. E., Panzenbeck, M. J., Kishimoto, T. K. & Giblin, P. A. (2003) *J. Immunol. Methods* **277,** 101–115
27. Bellosta, S., Ferri, N., Bernini, F., Paoletti, R. & Corsini, A. (2000) *Ann. Med.* **32,** 164–176
28. Veillard, N. R. & Mach, F. (2002) *Cell. Mol. Life Sci.* **59,** 1771–1786
29. Frenette, P. S. (2001) *N. Engl. J. Med.* **345,** 1419–1421
30. Youssef, S., Stuve, O., Patarroyo, J. C., Ruiz, P. J., Radosevich, J. L., Hur, E. M., Bravo, M., Mitchell, D. J., Sobel, R. A., Steinman, L. & Zamvil, S. S. (2002) *Nature* **420,** 78–84
31. Wekerle, H. (2002) *Nature* **420,** 39–40
32. Raggatt, L. J. & Partridge, N. C. (2002) *Drugs* **62,** 2185–2191